Chapter 18
Aquatic Colloids: Provenance, Characterization and Significance to Environmental Monitoring

Jae-Il Kim

Abstract Aquatic colloids are ubiquitous in all kinds of natural water and in general found to be small in size (<100 nm) and low in number density (<10^{14} particles per liter). Colloids of such properties may play a significant role for the aquifer migration of environmentally hazardous contaminants: radioactive elements as well as other trace chemical composites. Insightful knowledge on aquatic colloids is therefore perceived as indispensable for monitoring the environmental behavior of hazardous trace constituents.

This chapter describes the chemical process of generating aquatic colloids, e.g. their kernels like hydroxy aluminosilicate (HAS) colloids, as well as the incorporation of radionuclides into such colloid formation. Likely processes are characterized in particular by a combination of different nanoscopic approaches. The colloid formation is monitored radiochemically in conjunction with the highly sensitive spectroscopic speciation, e.g. time-resolved laser fluorescence spectroscopy (TRLFS), which facilitates the chemical characterization of trace actinides in particular. Colloids thus generated are quantified for their average size and number density by laser-induced breakdown detection (LIBD) upon optical plasma monitoring. Exemplary illustrations are summarized for the formation of colloid-borne trivalent actinides (Am, Cm), which become incorporated into HAS-colloids. Discussion is extended to the migration behavior of radionuclides as colloid-borne species in natural aquifer systems, for which a field experiment is chosen as a case in point.

Keywords: Aquatic colloids, speciation, actinides, migration, environmental monitoring

Institut für Nukleare Entsorgung (INE), Forschungszentrum Karlsruhe (FZK)
76021 Karlsruhe, Germany

Y.J. Kim and U. Platt (eds.), *Advanced Environmental Monitoring*, 233–247.

18.1 Introduction

Aquatic colloids are ubiquitous in all kinds of natural water (Yariv 1979; Bolt et al. 1991; Kim 1986, 1991, 1994). Their concentrations and size range vary widely depending on the geochemical surrounding of each given aquifer. Normally the particle size ranges from 1 nm up to 400 nm in average diameter but the particles of predominant number density are found as less than 100 nm (Kim et al. 2002). Number density (particles per liter water) varies from 10^{11} upwards over 10^{14} (Kim et al. 2002). Chemical composition of aquatic colloids is wide-ranging as maintained by their provenance (Yarif 1979; Bolt et al. 1991; Kim 1993). In general, they can be categorized into two different composites: inorganic colloids composed by heterogeneous polynucleation via oxo-bridging of different metal ions and organo–inorganic colloids produced by aggregation of inorganic colloids via complexation with organic molecules, e.g. humic acid (Bolt et al. 1991; Kim 1991; Malcolm and Bryan 1998). By nature they are hydrophilic, as exposed with the negatively charged surface, and thus play a carrier role for contaminant trace metal ions, e.g. radioactive elements like actinides, in aquifer systems (Artinger et al. 2002a,b; Hauser et al. 2002; Geckeis et al. 2004). Organic contaminants of polarized nature can also be carried on migration by inorganic colloids (Bolt et al. 1991).

Colloid-facilitated migration, especially, of trace actinide ions is of cardinal importance for the environmental monitoring in particular with respect to the radioecological safety aspect (Kim and Grambow 1999). It is to note that the radiochemical toxicity is attributed to radioelement concentrations that are much lower than concentration limitations of given elements for the chemical toxicity. For this reason, the long-term safety assessment of nuclear waste disposal entails the well-founded knowledge on aquatic colloids, on their interaction with trace radionuclides, above all long-lived actinides, and eventually on their migration behavior (Kim and Grambow 1999; Kim 2000).

This chapter is a brief summary review of recent investigations dealing with the provenance of aquatic colloids, the characterization as regards their interaction with trace actinide ions and the migration behavior of colloid-borne actinides. For this purpose, notable examples are selected to demonstrate how to characterize aquatic colloids with modern instrumentation, how to speciate the actinide interaction with colloids and how to appraise the colloid-facilitated migration of actinides in a given aquifer system. The subject matter under discussion may certainly be applicable to the environmental monitoring of other contaminants as well.

18.2 Aquatic Colloids in Nature

As natural water is always in contact with various mineral surfaces in a given geological formation, weathering products of surfaces are dispersed, dissolved and coagulated into new chemical composites, either hydrophobic states to precipitate

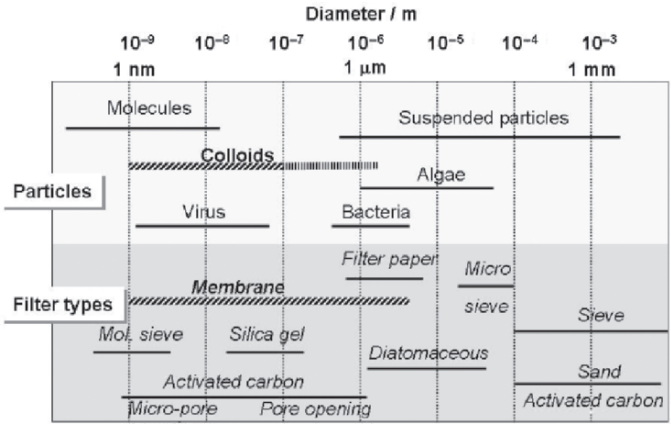

Fig. 18.1 Size ranges of various aquatic particles and pore openings

or hydrophilic states as colloids (Yarif 1979; Bolt et al. 1991). A colloidal fraction generated in such a process is often mixed with suspended particles of relatively large size (up to a few μm), which are prone to sedimentation with time; as a result, a stable fraction of colloids appears to be small in number density (10^{11}–10^{14} particles per liter, or over) as well as in average size (<100 nm) (Kim 1993; Kim et al. 2002). The particle size range of aquatic colloids can be compared with other aquatic particulates as shown in Fig. 18.1 (Stumm and Morgan 1981; Kim 1993). The size range of aquatic colloids is comparable with that of virus but evidently smaller than that of bacteria and microalgae. Sampling of subsurface water or groundwater induces often oxidation (e.g. Fe^{2+}) and decomposition of carbonate, thus leading to hydroxide of metal ions, as a result, produces suspended particles of larger size (Kim 1991). This kind of artifacts confuses in fact the particle size range of actual aquatic colloids. Therefore, the colloid size range is marked in Fig. 18.1 in two regions: actual range of <100 nm and uncertain range up to a few µm. Pore openings of various filter types (Stumm and Morgan 1981) are also given in this figure for the purpose of comparison. Modern membrane filters of different pore openings facilitate the size characterization of aquatic colloids, once careful precaution is attended to experimental handling.

An example of characterizing aquatic colloids in deep groundwater interwoven in various aquifer areas in Gorleben, northern Germany, is shown in Fig. 18.2 (Kim 1993). Colloids in this groundwater are composed of organo–inorganic composites, which contain a vast array of trace metal ions. The average size of predominant number density (10^{11}–10^{14} particles per liter) ranges <100 nm with a minor fraction up to 450 nm (Kim 1993). Colloid-borne concentrations of selected trivalent and tetravalent elements (homologues of actinides) are found to be a proportional function of the DOC (dissolved organic carbon) concentration, made mostly of fulvic and humic acids. All these elements are incorporated quantitatively into colloids. Age determination by ^{14}C-dating of humic components indicates these aquatic colloids

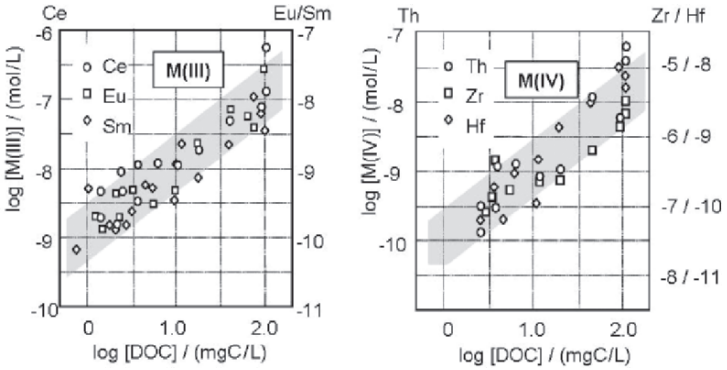

Fig. 18.2 Concentrations of water-borne trivalent and tetravalent trace elements associated with aquatic colloids as a function of the DOC (dissolved organic carbon, mostly humic and fulvic acids) in deep groundwater at Gorleben, Germany

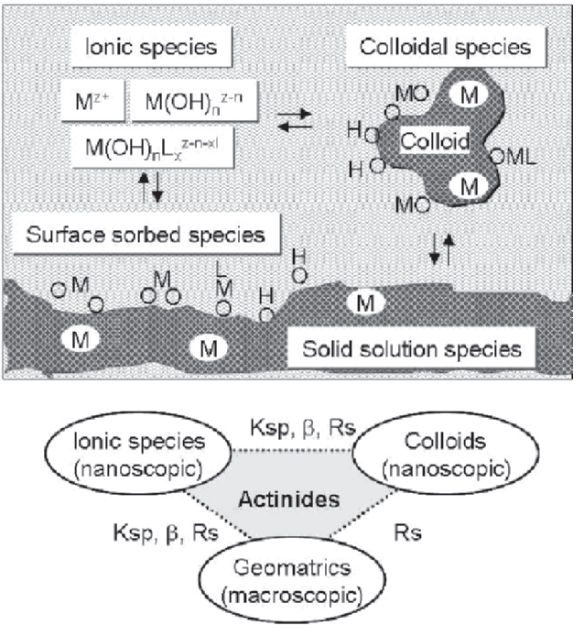

Fig. 18.3 A three phase system: ionic, colloid and solid, overruling the distribution of trace metal ions in aquifer systems

older than 20,000 years (Buckau et al. 2000). The fact suggests that aquatic colloids can remain stable for a long period.

Knowing that mineral-water interface systems add always in aquatic colloids (Bolt et al. 1991; Kim 1991), the environmental monitoring entails the appraisal of contaminant distributions into three different phases: ionic, colloid and solid (minerals) phases. Illustrations given in Fig. 18.3 demonstrate typical three phase interactions of

given metal ions that can be anticipated in aquifer systems (Kim and Grambow 1999). Specific reactions can be quantified separately between the two phases; ionic–colloid, ionic–solid and colloid–solid by assessing solubility products (Ksp), complexation constants (β) and partition ratios (Rs) for individual elements concerned. Such quantifications are, however, difficult, if not unfeasible, since necessary parameters to be taken into account are not always accessible straightforwardly (Kim 2000). Main difficulty arises in the characterization and quantification of aquatic colloids involved in a given system, namely particle size, number density and chemical composition. As aquatic colloids are relatively small in size and low in number density, conventional methods, like ultrafiltration, ultracentrifugation, light-scattering measurement etc., often fail in their proper quantification. As a response to such difficulty, a noble method has been introduced recently (Scherbaum et al. 1996; Bundschuh et al. 2001b), which is capable of quantifying aquatic colloids for their average size and number density in parallel. Discussion on this approach is briefly made here without commenting on other conventional methods, since they are handled multiply in the open literature (Ross and Morrison 1988).

18.3 Quantification of Aquatic Colloids by Laser-Induced Breakdown Detection

Principle of laser-induced breakdown detection (LIBD) can be appreciated by illustrations depicted in Fig. 18.4 (Kim and Walther 2006). Modulated laser light of high-energy intensity (irradiance) sorbed into a colloid particle incites ionization of

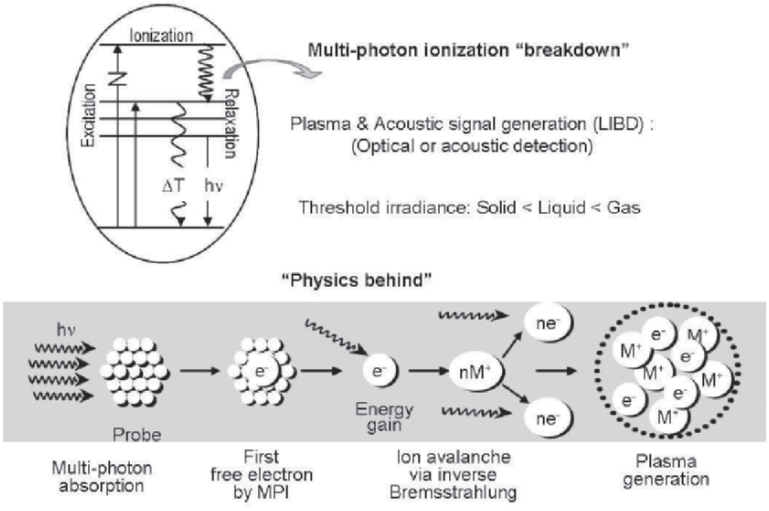

Fig. 18.4 An illustration of the laser-induced breakdown process for the determination of aquatic colloids

elements embraced therein. Energetic free electrons thus generated relax via giving off Bremsstrahlung that in turn creates further ionization and hence ion avalanche via so-called inverse Bremsstrahlung (Scherbaum et al. 1996; Walther et al. 2002; Kim and Walther 2006). Ignition of plasma takes place above the threshold irradiance for the physical state of a given prove, which follows: gas > liquid > sold. This principle makes selective detection of colloids in water possible. Consequently, the colloid particle undergoes "breakdown", leading to a nanoscopic plasma bundle. Whereas acoustic waves generated at the event of breakdown can be monitored by acoustic detection for determining number density (Scherbaum et al. 1996), the indiscrete relaxation of plasma can be monitored optically for a two-dimensional localization of plasma within the laser focus volume to ascertain an average size of colloids (Bundschuh et al. 2001b). Calibration of the latter process as a function of the laser beam irradiance enables monitoring both the average particle size and number density.

The particle detection sensitivity of LIBD, as calibrated by well-defined polystyrene reference particles, is compared with that of light scattering methods in Fig. 18.5: static and dynamic (PCS: photon correlation spectrometry) modes (Bundschuh et al. 2001b). As is apparent from this figure, the light scattering method is basically not sensitive enough for detecting colloids of small in size and low in number density, which is generally the case for aquatic colloids. On the other hand, LIBD is capable of detecting small colloids of very dilute concentrations, for which it is superior to light scattering by a factor of 10^4–10^7 in the predominant size range of actual aquatic colloids (indicated by gray shade).

Potential of LIBD is visualized, as shown in Fig. 18.6 (Bundschuh et al. 2001a), by monitoring colloids present in a variety of potable waters together with those in laboratory water from a Milli-Q apparatus. Non-processed tap water of the author's

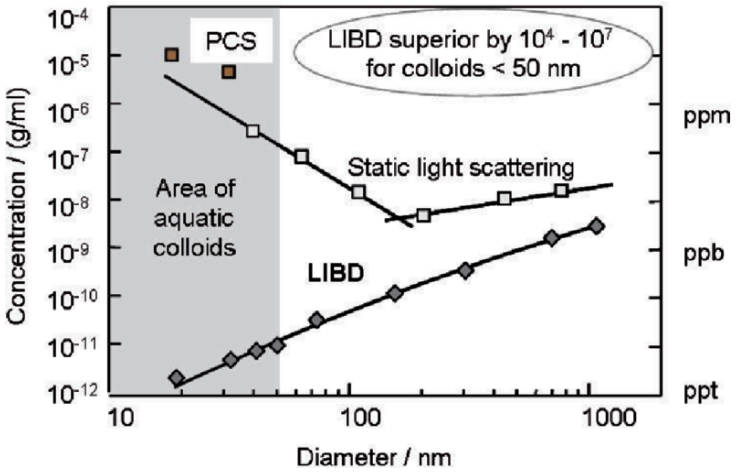

Fig. 18.5 Detection sensitivities of laser-induced breakdown detection (LIBD) in comparison with those of conventional light scattering methods

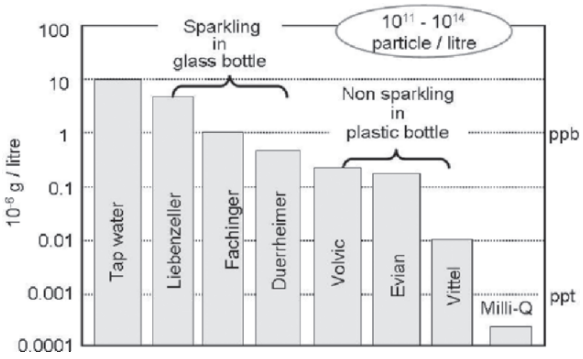

Fig. 18.6 Aquatic colloids present in various potable water

laboratory shows the highest colloid concentration compared to other bottled waters, reaching 10 µg/L (10 ppb). With a dominant particle size of <50 nm, the number density approaches to 10^{14} particle per liter. Non sparkling waters in plastic bottles contain less colloids than sparkling waters in glass bottles. Surface of glass bottles may be leached out with time, as a result, nanoscopic particles dispersed as colloids. The number density of colloids in potable water ranges in general from 10^{11} to 10^{14} particle per liter (Kim and Walther 2006). Fig. 18.6 corroborates simply the omnipresence of aquatic colloids. Provenance of such aquatic colloids is of keen interest to comprehend, above all, for appraising how the environmental monitoring can be advanced for trace actinides, of which the migration is eventually facilitated by aquatic colloids.

18.4 Provenance of Aquatic Colloids

Sound perception of how aquatic colloids are generated entails fundamental knowledge on prime kernels of their composition (Iler 1997; Kim et al. 2002). Following this trait, the major components of abundant aquifer minerals are sought out for the preliminary investigation. Aluminum and silicon oxides are dominant components in lithosphere (Pettijohn 1948; Mason 1952) and therefore, aluminosilicate composites become dominating aquifer minerals, much of which is clayey composition (Stumm and Morgan 1981; Bolt et al. 1991). Besides amorphous silicon oxide, most aluminosilicate minerals are sparingly soluble in the neutral pH range of water; the low solubility shores up on the other hand-dissolved species becoming colloidal. Some aluminosilicate minerals, together with amorphous silicon and aluminum oxides, are selected for illustrating their solubilities (Lindsay 1979; Stumm and Morgan 1981) as a function of pH in Fig. 18.7 (Kim et al. 2002). Relatively good soluble sillimanite and poorly soluble kaolinite and low albite are chosen for illustration. The near neutral pH range (indicated by gray shade), where solubilities

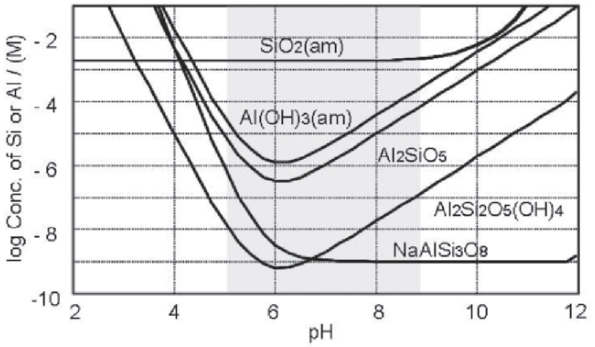

Fig. 18.7 Solubilities of amorphous silica and aluminum hydroxide, together with aluminosilicate composites: sillimanite (Al_2SiO_5), kaolinite ($Al_2Si_2O_5(OH)_4$) and low albite ($NaAlSi_3O_8$)

are low, appears to be the favorable condition for generating colloids in a composition of hydroxy aluminosilicates (HAS). They are kernels of aquatic colloids primarily. How such colloids incorporate trace actinides is an essential insight into the provenance of colloid-borne actinides in a given nuclear waste repository. Knowing that natural aquatic conditions are complex, owing to multiple interactions of a wide range of waterborne trace components: metal ions, either inorganic or organic anions, hydrophilic molecules etc. (Lindsay 1979; Stumm and Morgan 1981), this chapter concentrates only on a key feature for the formation of aquatic HAS-colloids as well as of colloid-borne actinides.

18.5 Generation of Aquatic Colloid-Borne Actinides

Hydroxy aluminosilicate (HAS) colloids are generated by mixing of acidic Al with alkaline Si to predisposed neutral pH in the presence of trivalent actinides, Am or Cm, in a trace concentration of 5×10^{-8} M (Kim et al. 2002). Am and Cm (chemical homologues) are alternately used for the reason that the former is on hand for a large-scale experiment, while the latter available only in a trace concentration is favored for the spectroscopic speciation (Panak et al. 2003). The Al concentration is varied from 10^{-3} M to 10^{-7} M (from over to under saturation, cf. Fig. 18.7), while keeping the Si concentration constant at 10^{-2} M (over saturation) and at 10^{-3} M (under saturation) for delivering polysilicic acid in the former and monosilicic acid in the latter (Kim 2005). Radiochemical measurements, after phase separation by a sequential ultrafiltration at two different pore openings: at 450 nm followed at 1 nm, make the evaluation of colloid fraction available, according to an empirical convention: *ionic species* < *1 nm* < *colloids* < *450 nm* < *precipitate* (Kim et al. 2002). In parallel, colloids are monitored directly by LIBD and visually by AFM (atomic force microscopy) (Kim et al. 2002). Both approaches give a comparable result:

an average size range of 10–50 nm for predominant particles. The number density determined by LIBD ranges 10^{11}–10^{14} particle per liter depending on the experimental condition applied, pH and initial concentrations of Al and Si.

Speciation of colloid-borne trivalent actinides is performed by time-resolved laser fluorescence spectroscopy (TRLFS) (Klenze et al. 1991), which provides the possibility of appraising excitation and relaxation spectroscopy as well as measuring the fluorescence lifetime of a probe elements concerned. Application of the three optical characteristics in parallel leads to chemical speciation with high sensitivity. To attain the high spectroscopic sensitivity, Cm(III) is chosen for the purpose of demonstrating the trivalent actinide behavior (Panak et al. 2003). Formation of colloid-borne Cm is surveyed as a function of pH along with the generation of HAS-colloids in a mixed solution containing 10^{-2} M Si (polysilicic acid prevails), 10^{-4} M Al and 5×10^{-8} M Cm. Three colloid-borne Cm species are identified (Kim et al. 2005), as illustrated in Fig. 18.8, which are named: Cm-HAS(I), Cm-HAS(II) and Cm-HAS(III). Increasing pH converts Cm-HAS(I) to CmHAS(II) and further to Cm-HAS(III) progressively. At pH 6 and beyond, Cm-HAS(III) becomes gradually prevailing, which remains stable in a period of over 60 days of observation. The similar experiment with 10^{-3} M Si (monosilicic acid prevails) results in the formation of Cm-HAS(I) and Cm-HAS(II) species only under the same experimental conditions (Panak et al. 2003).

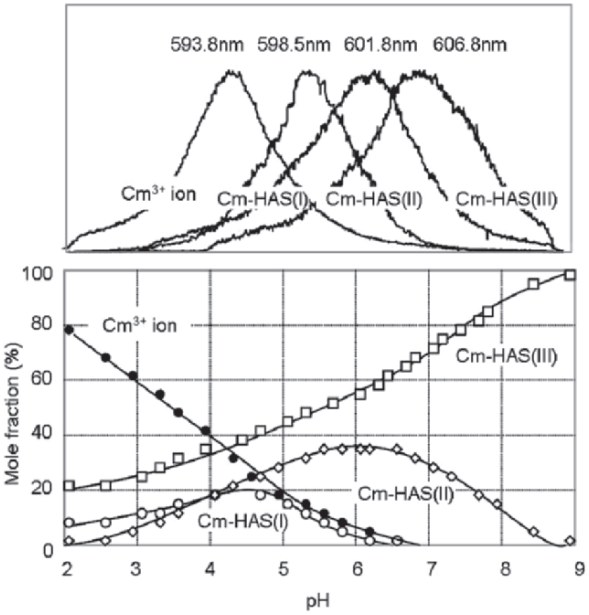

Fig. 18.8 Spectroscopic speciation of different HAS-colloid-borne Cm(III) species as a function of pH by time-resolved laser fluorescence spectroscopy (TRLFS). HAS denotes hydroxy aluminosilicate

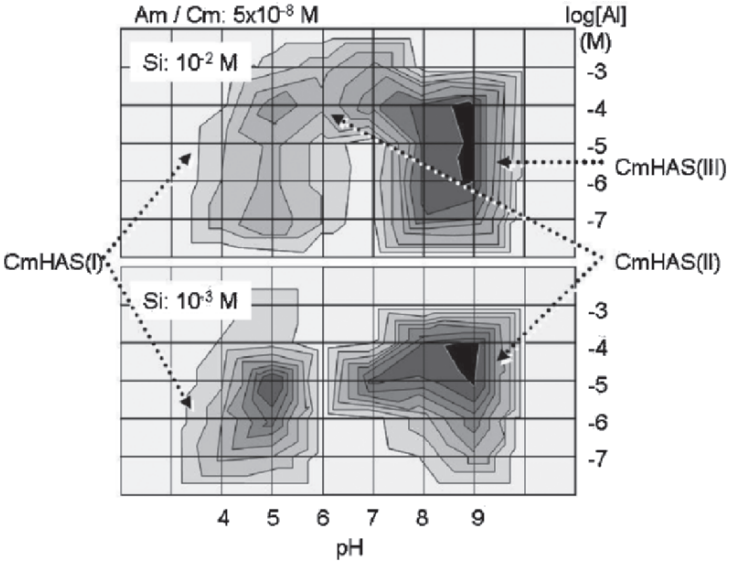

Fig. 18.9 Formation of HAS-colloid-borne Cm (or Am) at 10^{-2} M Si (polysilicic acid) and at 10^{-3} MSi (monosilicic acid) as a function of the Al concentration and pH. Contour areas are divided at a 10% interval of the colloid-borne Cm (or Am) fraction in solution (increasing gradually with darker shade)

A broad screening experiment is carried out radiochemically by adding 5×10^{-8} M Am in order to ascertain favorable conditions for the formation of colloid-borne actinides(III). The results are summarized in Fig. 18.9 as contour diagrams for the fractions of colloid-borne Am (Kim et al. 2005). Since Am and Cm are chemically homologues in solution, Figs. 18.8 and 18.9 can be correlated with each other. Correlation of the two figures, together with the speciation results of Cm-HAS formation at 10^{-3} M Si (Kim et al. 2002: not shown here), makes distinction of favorable experimental conditions for generating each of HAS-colloid-borne Am (or Cm). Colloidal species of Cm-HAS(I) is formed only at low pH, Cm-HAS(II) in 10^{-3} M Si at high pH or in 10^{-2} M Si around pH 6 and Cm-HAS(III) only in 10^{-2} M Si at pH >7.

The fluorescence relaxation time of each colloid-borne Cm species is found to be different from one another, following the order of Cm-HAS(I) < Cm-HAS(II) < Cm-HAS(III) (Kim et al. 2005). Resolving the relaxation time, the hydration number of water molecules bound to each Cm in HAS-colloids is found: 7 H_2O to Cm-HAS(I), 6 H_2O to Cm-HAS(II) and 0/1 H_2O to Cm-HAS(III) in relation to the reference value of 8/9 H_2O coordinated to the aqueous Cm^{3+} ion (Kim et al. 2005). According to these results, the chemical structure of each HAS-colloid-borne Cm species can be postulated as shown in Fig. 18.10. Based on the results discussed hitherto, it is possible to draw a conclusion that, in the formation process of HAS-colloids, trace trivalent actinides are incorporated by surface sorption

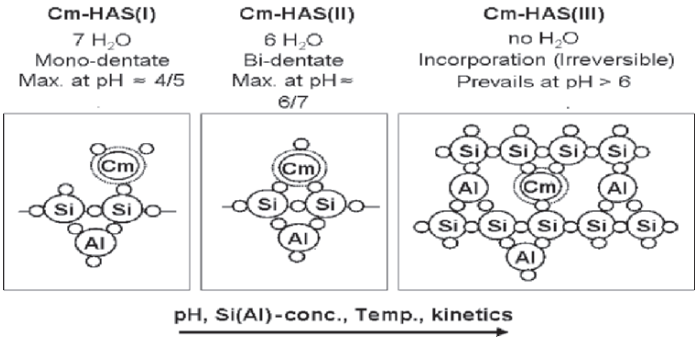

Fig. 18.10 Chemical states postulated based on the fluorescence lifetime of each HAS-colloid-borne Cm species: a conversion of the species takes place with increasing pH, the concentration of Si (Al) and temperature from left to right

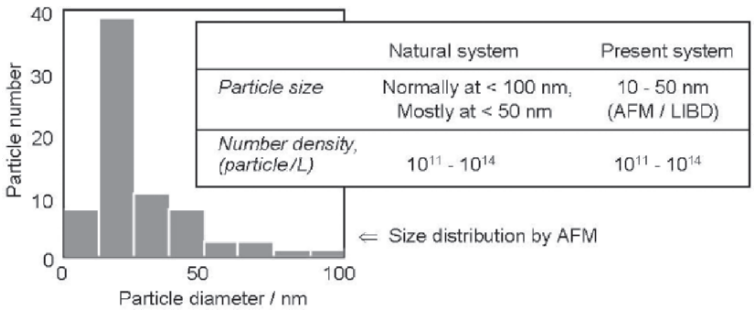

Fig. 18.11 A particle size distribution of HAS-colloids determined by AFM; average size and number density ranges ascertained by LIBD for natural aquatic colloids and HAS-colloids

as well as by coalescing into the colloidal structure, substituting Cm (or Am) at the Al site. The latter process generates a stable HAS-colloid-borne Cm (or Am), i.e. Cm-HAS(III) colloids. Characterization of such stable colloids made by LIBD and AFM leads to the results given in Fig. 18.11 (Kim et al. 2002). The average size and number density of HAS-colloids vary obviously with experimental conditions, e.g. pH, the concentration of each component involved.

Summarizing the so far discussed results and according the atomic ratio found as approximately 1 for Al/Si (Kim et al. 2002) in the HAS composition, the formation of HAS-colloids can be described as follows:

$$nAl(OH)_{3-y}^{y+} + Si_{n-1}(OH)_{2n-2} \Leftrightarrow Al_nSi_nO_{4n-2-x}(OH)_x^{x-n-4} + (7+ny-x)H^+ + (2n-ny-1)H_2O$$

In this reaction an isomorphic substitution of trivalent trace actinides to Al may take place as depicted in Fig. 18.10 (right side). The reaction is pH reversible and hence a conversion of HAS-colloid-borne Cm species takes place as shown in Fig. 18.8.

18.6 Migration Behavior of Colloid-Borne Actinides

Aquatic colloids generate evidently colloid-borne actinides as exemplified by the aforementioned example, which are called pseudocolloids of actinides (Kim 1991). Further, the migration behavior of colloid-borne actinides is of cardinal importance for the environmental monitoring, in other words, for the safety assessment of nuclear (or other) waste disposal (Kim and Grambow 1999; Kim 2000). In natural aquifer systems, pore-openings are in general large enough for unconstrained waterway of aquatic colloids as can be appreciated from Fig. 18.12. The migration behavior of actinides (as well as other contaminants) in a given aquifer system can be assessed by monitoring the retardation coefficient (R_f) of given ions, molecules or colloids. R_f represents a ratio of the migration velocity of a waterborne component vs. the water flow velocity (Kim and Grambow 1999). The migration process is depicted in Fig. 18.12 for waterborne components (e.g. ionic radionuclides [RN])

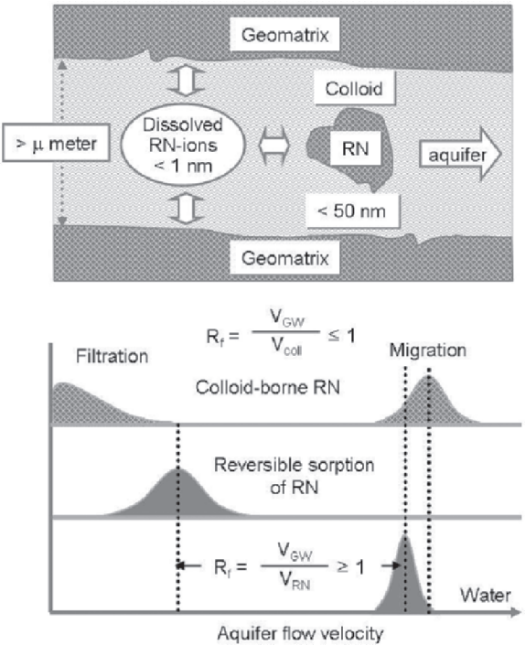

Fig. 18.12 An illustration of the migration behavior of radionuclides in ionic species interacting with mineral surfaces and in colloidal form devoid of interaction

undergoing surface interactions as well as for colloid-borne RN, which appears to be least interacting. Surface interactions result in the R_f value larger than one always, whereas the migration of colloids, devoid of interaction, is enhanced by advection to a certain extent and hence R_f becomes slightly less than one (Artinger et al. 2002a,b). Consequently, aquatic colloids facilitate the migration of actinides only. On the other hand, non-colloidal actinide ions are prone to sorption onto aquifer mineral surfaces, thus immobilized easily, as noticed by significantly large R_f values (Mckinley and Scholtis 1993; Vandergraaf et al. 1993).

The colloid-facilitated migration of actinides is observed in a field experiment. The field-laboratory in Grimsel, Switzerland, which has been built up for the investigation of the nuclear waste disposal safety, is chosen for the migration experiment of colloid-borne actinides (Hauser 2002, Geckeis 2004). Bentonite colloids (average diameter <200 nm; smectite type) dispersed in in situ granite water are spiked by trace concentrations of trivalent and tetravalent actinide homologue ions: Th(IV), Hf(IV) and Tb(III) (Hauser 2002). To a water passage of 5 m granite fracture distance, aquatic colloids are injected by air pressure at one end and extracted at another end. The experiment is visualized in Fig. 18.13. The colloid migration is monitored in-situ by LIBD for their concentration and average size in input and output waters. Colloid-borne elements are analyzed afterward by ICP-MS in laboratory. Migration profiles summarized in Fig. 18.13 (inset) indicate that the

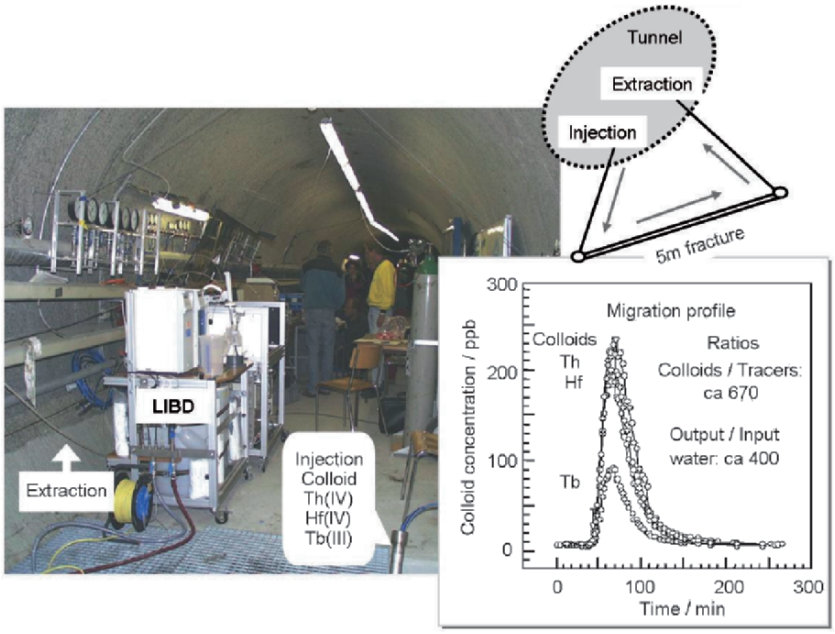

Fig. 18.13 A field experiment of the colloid-borne actinide (homologues) migration in the Grimsel, Switzerland underground laboratory (tunnel) for a 5 m distance of the granite fracture. Trace metal ions are accompanied by bentonite colloids of <200 nm

migration of trivalent and tetravalent elements is facilitated by aquatic colloids. Recovery of tetravalent Th and Hf amounts to about 75% and of trivalent Tb to about 35% (Hauser et al. 2002). Improvement of spiking metal ions onto colloids in the subsequent experiment results in a near quantitative recovery of all trace elements introduced (Geckeis et al. 2004). Both laboratory and field experiments (Artinger et al. 2002a,b; Hauser et al. 2002; Geckeis et al. 2004) substantiate that the actinide migration is facilitated by aquatic colloids, which thus play as a carrier role.

18.7 Final Remarks

The colloid-facilitated migration of actinides has been investigated by laboratory experiments as well as by field experiments. All these endeavors have corroborated that actinides become migrational only in accompany with aquatic colloids. Therefore, fundamental knowledge on aquatic colloids and their provenance is an essential prerequisite for the radioecological monitoring and also for the environmental monitoring of other contaminants. This is particularly true for the long-term safety assessment of nuclear waste disposal. However, not much is known for the provenance of colloid-borne actinides, i.e. geochemical processes of such colloid formation, because of experimental difficulties involved in the appraisal of nanoscopic reactions. Limitation of space allocated for this chapter renders summarizing only some notable examples from the recent investigations in this subject field.

References

Artinger R., Schuessler W., Scherbaum F., Schild D., and Kim J.I. (2002a), Am-241 migration in a sandy aquifer studied by long-term column experiments. *Environ. Sci. Technol.,* 36, 4818–4823.

Artinger Rabung T., Kim J.I., Sachs S., Schmeide K., Heise K.H., Bernhard G., and Nitsche H. (2002b), Humic colloid-borne migration of uranium in sand columns, *J. Contam. Hydrol.,* 58, 1–12.

Bolt G.H., De Boodt M.F., Hayes M.H.B., and McBride M.B. (1991), *Interact. Soil Colloid-Soil Solut*., Kluwer Academic Publishers, Dordrecht, The Netherlands.

Buckau G., Artinger R., Geyer S., Wolf M., Fritz P., and Kim, J.I. (2000), C-14 dating of Gorleben groundwater. *Appl. Geochem.,* 15, 583–597.

Bundschuh T., Knopp R., and Kim, J.I. (2001a), Laser-induced breakdown detection of aquatic colloids with different laser systems. *Colloids and Surfaces A: Physicochem. Eng. Asp.,* 177, 47–55.

Bundschuh T., Hauser W., Kim J.I., Knopp R., and Scherbaum F.J. (2001b), Determination of colloid size by 2-D optical detection of laser-induced plasma. *Colloids and Surfaces A: Physicochem. Eng. Asp.,* 180, 285–293.

Geckeis H., Schäfer T., Hauser W., Rabung T., Missana T., Degueldre C., Mori A., Eikenberg J., and Fierz T. (2004), Results of the colloid and radionuclide retention experiment (CRR) at the

Grimsel test site, Switzerland: Impact of reaction kinetics and speciation on radionuclide migration. *Radiochim. Acta*, 92, 765–774.

Hauser W., Geckeis H., Kim J.I., and Fierz T. (2002), A mobile laser-induced breakdown detection system and its application for the in situ monitoring of colloid migration. *Colloids and Surfaces A: Physicochem. Eng. Asp.,* 203, 37–45.

Iler R.K. (1997), *The Chemistry of Silica*. Wiley-Interscience, New York.

Kim J.I. (1986), Chemical behavior of transuranic elements in natural aquifer systems. In *Handbook on the Physics and Chemistry of the Actinides*, A. J. Freeman and C. Keller, (eds.), Elsevier Science Publishers, B. V., Amsterdam, New York, chap. 8, 413–455.

Kim J.I. (1991), Actinide colloid generation in groundwater. *Radiochim. Acta*, 52–53**,** 71–81.

Kim J.I. (1993), The chemical behavior of transuranium elements and barrier functions in natural aquifer systems. *Mat. Res. Symp. Proc*., 294, 3–21.

Kim J.I. (1994), Actinide colloids in natural aquifer systems. *MRS Bull.,* 19(12), 47–53.

Kim J.I. and Grambow B. (1999), Geochemical assessment of actinide isolation in a German salt repository environment. *Eng. Geol.,* 52, 221–230.

Kim J.I. (2000), Is the thermodynamic approach appropriate to describe natural dynamic systems (status and limitations). *Nucl. Eng. Des.,* 202, 143–155.

Kim M.A., Panak P.J., Yun J.I., Kim J.I., Klenze R., and Köhler K. (2002), Interaction of actinides with aluminosilicate colloids in statu nascendi, Part 1: generation and characterization of actinide(III) pseudocolloids. *Colloids and Surfaces A: Physicochem. Eng. Asp.,* 216, 97–108.

Kim M.A., Panak P.J., Yun J.I., Priemyshev A., and Kim J.I. (2005), Interaction of actinides(III) with aluminosilicate colloids, in statu nascendi, Part III: Colloid formation from monosilanol and polysilanol. *Colloids and Surfaces A: Physicochem. Eng. Asp.,* 254, 137–145.

Kim J.I. and Walther C. (2007), Laser-induced breakdown detection. In *Environmental Colloids and Particles: Behaviour, Separation and Characterisation.* Wilkinson K.J. and Lead J.R (Eds) chap. 12, Wiley & Sons, London, 555–612.

Klenze R., Kim J.I., and Wimmer H. (1991), Speciation of aquatic actinide ions by pulsed laser spectroscopy. *Radiochim. Acta*, 52–53, 97–103.

Lindsay W.L. (1979), *Chemical Equilibria in Soils*, Wiley, New York.

Malcolm N. and Bryan N.D. (1998), Colloidal properties of humic substances. *Adv. Colloid Interfac.,* 78, 1–48.

Mason B. (1952), *Principles of Geochemistry*, Wiley, New York.

McKinley I.G. and Scholtis A. (1993), A comparison of radionuclide sorption databases used in recent performance assessments. *J. Contam. Hydrol.,* 13, 347–363.

Panak P.J., Kim M.A., Yun J.I., and Kim J.I. (2003), Interaction of actinides with aluminosilicate colloids in statu nascendi, Part 2: spectroscopic speciation of colloid-borne actinides(III). *Colloids Surf. A: Physicochem. Eng. Asp.,* 227, 93–103.

Pettijohn F.J. (1948), *Sedimentary Rocks*, Harper and Brothers, New York.

Ross S. and Morrison I.D. (1988), *Colloidal Systems and Interfaces*, Wiley, New York.

Scherbaum F.J., Knopp R., and Kim J.I. (1996), Counting of particles in aqueous solutions by laser-induced photoacoustic breakdown detection. *Appl. Phys. B: Lasers Opt*., 63, 299–306.

Stumm W. and Morgan J.J. (1981), *Aquatic Chemistry*, Wiley, New York.

Yariv S and Cross H. (1979), *Geochemistry of Colloid System*, Springer-Verlag, Berlin.

Vandergraaf T.T., Ticknor K.V., and Melnyk T.W. (1993), The selection of a sorption database for the geosphere model in the Canadian nuclear fuel waste management program. *J. Contam. Hydrol.,* 13**,** 327–345.

Walther C., Bitea C., Hauser W., Kim J.I., and Scherbaum F.J. (2002), Laser induced breakdown detection for the assessment of colloid mediated radionuclide migration. *Nucl. Instr. Meth. Phys. Res. Section B*, 195, 374–388.